Research Article

Modeling and Simulation of Multi Purposes Concentrated Solar Power System

K. A. Abed*, Amr M. A. Amin**, Adel A. El-Samahy** and Abdullah M. A. Shaaban*

*Mechanical Eng. Depart., National Research Centre (NRC).
**Electrical Eng. Depart., Faculty of Engineering, Helwan University*
_____

ABSTRACT

The investigated plant consists of solar collector field of 120 kW peak thermal capacity, thermal storage tank with 3 tons of therminol-66 oil, an Organic Rankine Cycle (ORC) of 4.3 kW nominal electric power production capacity, and thermally driven absorption chiller (TDC) of 35 kW cooling capacity. The present work aims to manage the thermal energy stored from Concentrated Solar Power (CSP) plant, in order to obtain the optimum operating condition of CSP System (ORC and TDC).
The system was modeled mathematically and simulated using Engineering Equation Solver (EES) software program in order to analyze the performance at similar conditions to the real ones to ensure the feasibility of the presented study. The present simulation program is loaded by the data of Donghong Wei et al [10] and the output results are compared. From this comparison between the present work and [10] for the output net power versus exhaust mass flow rate work, it is clear that, the two curves have the same trend with some acceptable deviations. The output results were analyzed. Effect of hot oil temperature and mass flow rate on ORC output and efficiency are investigated. Also effect of generator and evaporator temperatures on TDC cooling capacity and coefficient of performance are obtained. At optimum operating condition, the electrical net output power from ORC is about 24 kW, while the TDC cooling capacity is about 24 kW. The optimum operating conditions occurs when 73.33 % from stored thermal energy is used for ORC and 26.67 % is used for TDC.

Key words: Renewable Energy, Concentrated Solar Power System, Organic Rankine Cycle, Thermally Driven Absorption Chiller
_____

1. INTRODUCTION

Nowadays, energy is one of the most basic and crucial elements upon which to base a life and an economy. Energy is very important for daily tasks in homes, schools, hospitals, business, transport applications, industries and countless other places. Most of energies come from burning fossil fuels like oil, coal and natural gas which are called conventional or traditional energy resources. These conventional resources pollute the environment, run out and their costs are in continuous increase since 1970's [1]. Since crisis for USA of the mid 1970's, the world's industrialized nations look at renewable energy sources (RES) as a supplement to providing the projected increase in energy demand in their nations in addition to increase awareness of the effects of emissions from fossil fuel power plants to the humans and environment. Governments in industrial countries are currently made debating and enacting pollution control regulations into laws [2].

Solar energy is a source, which can be exploited in two main ways to generate power: direct conversion into electric energy using photovoltaic panels and by means of a thermodynamic cycle. In CSP plants it is the sun's thermal energy to be stored, whereas in PV applications it is the electrical energy to be stored in batteries, although this is not economically and environmentally feasible in large-scale power plants. Umberto Desideri et al studied the performance of concentrated solar power plants equipped with molten salts thermal storage to cover a base load of 3 MWel. The electricity production of the CSP facilities has been analyzed and then compared with the electricity production of PV plants. Two different comparisons were done, one by sizing the PV plant to provide the same peak power and one using the same collectors' surface [3]. An economic analysis based on the estimation of the levelized electricity cost (LEC) for

_____

both CSP and PV power plants located both in south of Italy and Egypt was carried out in order to investigate which is the most cost effective solution [1]. In all the cases considered, the CSP facilities resulted the best option in terms of cost of electricity produced due to the continuity of energy production during the night hours.

Investigational dynamic simulations of an existing 50 MWel parabolic trough solar thermal power plant in Spain are carried out during clear days and slightly cloudy periods [4]. Wisam Abed et al present a dynamic model of a parabolic trough power plant. Besides the thermal energy storage system and solar field, the developed model describes the heat transfer fluid and steam/water paths in detail. Advanced control circuits, including drum level, economizer water bypass, at temperator and steam bypass controllers are also included. The parabolic trough power plant is modeled using Advanced Process Simulation Software (APROS). Wisam Abed et al get that, Firstly during summer days, the plant typically operates for 10–12 hr a day on solar energy at full-rated electric output. Furthermore, the thermal storage system enables the parabolic trough power plant to produce a constant electrical power rate, despite the slight fluctuations in the solar radiation. Secondly the thermal storage system after sunset continues approximately 7.5 hr for covering electrical power of 48 MWel until the thermal storage energy is completely depleted.

Organic Rankine Cycle coupling with a Parabolic Trough Solar Power Plant for cogeneration and industrial processes [5], in this work we present a study of a small CSP plant coupled to an ORC with a novel configuration since useful energy is directly used to feed the power block and to charge the thermal storage. In order to analyze this novel configuration we consider a case study with cogeneration applied to textile industrial process at medium temperature. It turns out that this configuration reduces the size of the thermal storage disposal. The performance of the solar power plant was simulated with TRNSYS to emulate real operating conditions. In order to increase the solar fraction and to improve the system it is worth to extend the study to more storage technologies. Molten salts could be a very good possibility to highly increase the solar fraction but it is much more expensive. On the other hand concrete storage is much cheaper but with less heat capacity. However phase change materials may be a good and interesting candidate with a balanced compromise between heat capacity and price.

Performance of a Single Effect Solar Absorption Cooling System (Libr-H2O) [6], many works were done to evaluate the performances of a solar cooling system working in water- lithium bromide pair. In 2012Rosiek, evaluated the performance of a solar-assisted 70 kW single effect LiBr-Water chiller located in Spain and achieved a maximum COP of 0.6 and Ali, assessed the performance of a 35 kW solar absorption cooling plant and reported maximum collectors' field efficiency of 49.2% and a COP of 0.81. Hammad and Zurigat, described the performance of a 1.5 Ton solar cooling unit. The unit comprises a 14 m² flat plate solar collector system and five shell and tube heat exchangers. The unit was tested in April and May in Jordan. The maximum value obtained for actual coefficient of performance was 0.85.In 2013, G. Cascales, studied the global modeling of an absorption system working with LiBr/H2O assisted by solar energy. It satisfies the air-conditioning necessities of a classroom in an educational center in Puerto Lumbreras, Murcia, Spain. The absorption system uses a set of solar collectors to satisfy the thermal necessities of the vapor generator. A dynamic simulation model, for a solar powered absorption cooling system was developed, and validated using measured data. Yeung and al., designed and installed a solar driven absorption chiller at the University of Hong Kong, this system included 4.7 kW absorption chiller, flat plate solar collectors with a total area of 38.2 m², water storage tank and the rest of the equipment. They reported that the collector efficiency was estimated at 37.5%, the annual system efficiency at 7.8% and an average solar fraction of 55%, respectively.

From the previous survey which includes some of the prior art for the work on concentrated solar power and storage the collected thermal energy to produce electrical power or for cooling load. Most studies work about either concentrated solar power in general or one of the electricity generation by ORC and cooling by absorption chiller. Concentrated solar power system which contains thermal energy storage system, organic rankine cycle, and thermal absorption chiller is very important. So, the present work aims to get the mathematical modeling of the system and simulating it on EES software.

2. MATHEMATICAL MODELING OF THE SYSTEM

Mathematical modeling is a representation in mathematical terms of the behavior of real devices and objects we want to know how to make or generate mathematical representations or models, how to validate them, how to use them, and how and when their use is limited. Since the modeling of devices and phenomena is essential to both engineering and science, engineers and scientists have very practical reasons for doing mathematical modeling. In addition, engineers, scientists, and mathematicians want to experience the sheer joy of formulating and solving mathematical problems.

2.1. Organic Rankine Cycle Modeling

The organic Rankine cycle is consists of an evaporator, a condenser, a pump and a turbine. From state 1 to 2, an ideal pump executes an adiabatic, reversible (isentropic) process to raise the working fluid from the condenser pressure to the evaporator pressure. From state 2 to state 3, an evaporator heats the fluid at a constant pressure (isobar transformation)

moving from a saturated liquid state 2' to a saturated vapor state 3' where all the liquid becomes vapor. Then the fluid is superheated until it reaches the state 3. After, the superheat vapor fluid enters in a turbine where it produces expansion through an adiabatic and reversible process. The superheat process is necessary in order to guarantee that in the turbine only vapor is present, this preserving the turbine blades from condensation and erosion. However, the amount of superheat should be kept as low as possible in order to avoid waste of energy and maximize the performance of the entire cycle. The typically used working fluid is an organic fluid which is characterized by low latent heat and high density. These properties are useful to increase the turbine inlet mass flow rate. Common working fluids that can be used are R-123, R-134a and R-245fa. The properties of the working fluid have a significant impact on the performance of the ORC cycle. The appropriate working fluids properties can lead to a higher cycle performance [7].

Modeling of the ORC is based on modeling of all components forming the cycle as shown in figure 1. The evaporator and the condenser were treated as a heat exchanger. The turbine and pump were simulated with isentropic process the components parameters were selecting for the available component in the market.
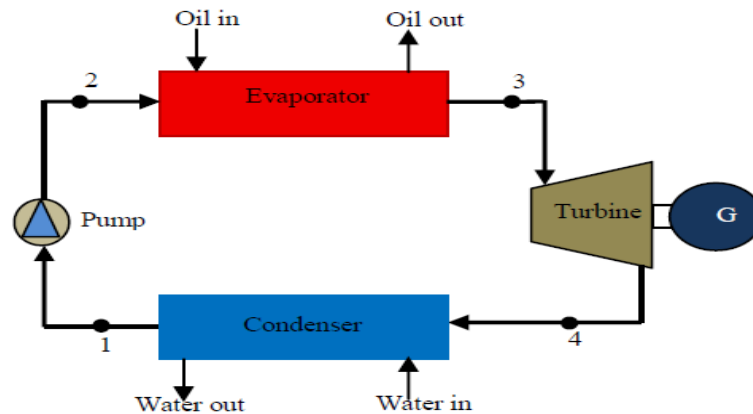

Fig. 1 Schematic diagram of the storage tank with segments [7]

One-dimensional heat transfer was assumed between the two heat transfer fluids. The thermal oil represents the heating source fluid which flow in the evaporator as one phase flow, while the organic fluid represents the cold fluid and pass through the evaporator in the different three phases (liquid, two phase and vapor phase). So that, the evaporator was divided to three main sections which are the liquid, two phase and the vapor sections each section was related as a separated heat exchanger. As heat losses in heat exchangers are neglected, the amount of the heat added to the working fluid in time is equal to the heat extracted from the heat source.

In general, for each zone the inlet temperature for the hot and the cold fluid stream are $T_{h,i}$ and $T_{c,i}$, respectively, and the outlet temperature for hot and cold streams are $T_{h,o}$ and $T_{c,o}$, respectively. The outlet fluids temperatures were calculated from the following equation [7]:

$$Q = m_h \, Cp_h \left(T_{h,i} - T_{h,o}\right) = m_c \, Cp_c \left(T_{c,o} - T_{c,i}\right) \qquad (1)$$

Where:

        Q: The actual heat transfer rate (kW).
        m_h: The mass flow rates of the hot fluid (kg/s)
        m_c: The mass flow rates of the cold fluid (kg/s)
        Cp_h: The specific heat of the hot fluid (kJ/kg k)
        Cp_c: The specific heat of the hot fluid (kJ/kg k)

The working fluid heated in the evaporator to superheated vapor at constant pressure (evaporating pressure). The heat transfer rate from the evaporator (Q_e) into the working fluid is given by:

$$Q_e = m_f(h_3 - h_2) = m_f Cp_f(T_3 - T_2) \qquad (2)$$

Where,

m_f : is the mass flow rate of the working fluid (kg/s)
h_3, h_2: is the enthalpy at points 3 and 2 (kJ/kg)
T_3, T_2: is the Temperature degree at points 3 and 2 (K)
Cp_f: is the specific heat of the working fluid (kJ/kg K)

The superheated vapor working fluid passes through the turbine to generate the mechanical power. Firstly, we can calculate the enthalpy at point 4 from the following equation (Assume Isentropic):

$$\eta_{turbine} = \frac{h3-h4}{h3-h4s} = \frac{T3-T4}{T3-T4s} \qquad (3)$$

_____

Where,

η_{turbine} : is the turbine efficiency

h_4: is the actual enthalpy at (kJ/kg)

T_4: is the actual Temperature degree at (K)

h_{4s}: is the isentropic enthalpy at (kJ/kg)

T_{4s}: is the isentropic Temperature degree at (K)

Then, the power output from the (W_t) turbine is given by:

$$W_t = m_{\dot{f}}(h_3 - h_4) = m_{\dot{f}}Cp_f(T_3 - T_4) \tag{4}$$

The exhaust vapor exits the turbine to the condenser where it is condensed by cooling water. The heat rate removed by the condenser (Q_c) can be expressed as:

$$Q_c = m_{\dot{f}}(h_4 - h_1) = m_{\dot{f}}Cp_f(T_4 - T_1) \tag{5}$$

Where,

h_1: is the enthalpy at point 1(kJ/kg)

T_1: is the temperature at point 1 (K)

The pump power (Wp) can be expressed as: (Assume Isentropic)

$$W_P = m_{\dot{f}}(h_2 - h_1) = m_{\dot{f}}Cp_f(T_2 - T_1) \tag{6}$$

To get the pump efficiency η_{pump}

$$W_p \cong m_{\dot{f}} \frac{\upsilon_1 \Delta P}{\eta_{\text{pump}}} \cong m_{\dot{f}} \frac{\upsilon_1(P2-P1)}{\eta_{\text{pump}}} \tag{7}$$

Where:

P2, P1: is the pressure at points 1 and 2 (kPa).

υ_1: is specific volume at point 1 (m^3/kg).

Finally, the system efficiency η_{ORC} is calculated as following:

$$\eta_{\text{ORC}} = \frac{W_t - W_p}{Q_e} \tag{8}$$

So, the gross electric power of the ORC unit ($W_{e,\text{gross}}$) is calculated as following:

$$W_{e,\text{gross}} = \eta_{\text{ORC}} Q_{\text{HEX}-\text{ORC}} \tag{9}$$

Where:

$Q_{\text{HEX}-\text{ORC}}$ is the thermal power provided at the ORC unit evaporator from the storage tank [9]

2.2. Thermal Absorption Chiller Modeling

With reference to the numbering system shown in figure 2, at point (1), the solution is rich in refrigerant and a pump (2) forces the liquid through a heat exchanger to the generator (3). The temperature of the solution in the heat exchanger is increased. In the generator, thermal energy is added and the refrigerant boils off the solution. The refrigerant vapor (7) flows to the condenser, where heat is rejected as the refrigerant condenses. The condensed liquid (8) flows through a flow restrictor to the evaporator (9). In the evaporator, the heat from the load evaporates the refrigerant, which flows back to the absorber (10). A small portion of the refrigerant leaves the evaporator as liquid spillover (11). At the generator exit (4), the fluid consists of the absorbent–refrigerant solution, which is cooled in the heat exchanger. From points (6)-(1), the solution absorbs refrigerant vapor from the evaporator and rejects heat through a heat exchanger [8].
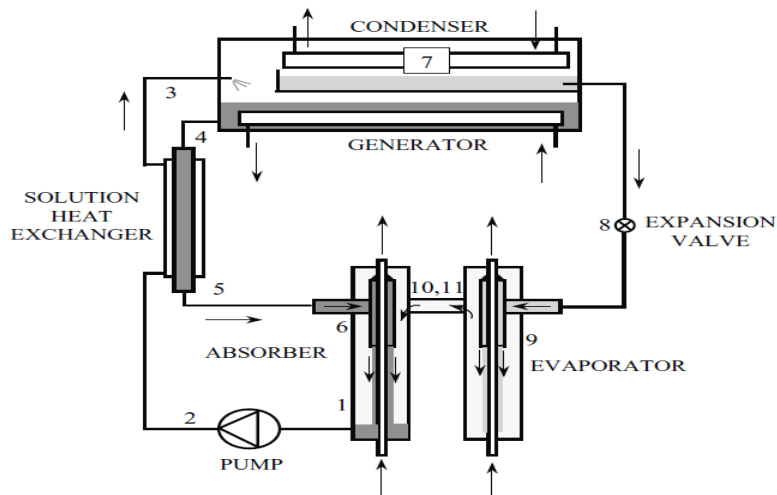

Fig. 2 Single effect, LiBr–water absorption cycle. [8]

_____

To perform estimations of equipment sizing and performance evaluation of a single-effect LiBr–water absorption cooler, basic assumptions and input values must be considered. With reference to figure 2, the basic assumptions are:

1. The steady state refrigerant is pure water.
2. There are no pressure changes except through the flow restrictors and the pump.
3. At points 1, 4, 8 and 11, there is only saturated liquid.
4. At point 10, there is only saturated vapor.
5. Flow restrictors are adiabatic.
6. The pump is isentropic.
7. There are no jacket heat losses.

Since, in the evaporator, the refrigerant is saturated water vapor and the temperature (T_{10}) is assumed, the saturation pressure at point 10 (P_{10}), as calculated from curve fit, and the enthalpy (h_{10}). Since, at point 11, the refrigerant is saturated liquid; its enthalpy can be calculated. The enthalpy at point 9 is determined from the throttling process applied to the refrigerant flow restrictor, which yields that $h_9=h_8$. To determine h_8, the pressure at this point must be determined. Since, at point 4, the solution mass fraction x_4 is an input value and the temperature at the saturated state was assumed, we can get the saturation pressure P_4 and h_4. Considering that the pressure at point 4 is the same as in point 8; then h_8 and h_9 can be obtained.

Once the enthalpy values at all ports connected to the evaporator are known, mass and energy balances can be applied to give the mass flow of the refrigerant and the evaporator heat transfer rate.

The mass balance on the evaporator is:

$$m_9 = m_{10} + m_{11} \tag{10}$$

The energy balance on the evaporator is:

$$Q_e = m_{10}h_{10} + m_{11}h_{11} - m_9h_9 \tag{11}$$

Where:

m_9, m_{10}, m_{11}: The mass flow rate at points 9, 10, and 11 (kg/s).

h_9, h_{10}, h_{11}: The enthalpy at points 9, 10, and 11 (kJ/kg).

Since the evaporator output power Q_e and Liquid carryover from evaporator m_{11} as a percentage of m_{10} were assumed, the mass flow rates can be calculated.

Since the values of m_{10} and m_{11} are known, mass balances around the absorber give:

$$m_1 = m_{10} + m_{11} + m_6 \tag{12}$$

and

$$x_1 m_1 = x_6 m_6 \tag{13}$$

The mass fractions x_1 and x_6 are inputs, and therefore m_1 and m_6 (mass flow rate at points 1 and 6 respectively) can be calculated. The heat transfer rate in the absorber can be determined from the enthalpy values at each of the connected state points. At point (1), the enthalpy (h_1) is determined from the input mass fraction x_1 is an input value and the assumption that the state is saturated liquid at the same pressure as the evaporator (P_{10}). The enthalpy value at point 6 (h_6) is determined from the throttling model, which gives $h_6 = h_5$.

The enthalpy at point 5 is not known but can be determined from the energy balance on the solution heat exchanger, assuming an adiabatic shell as follows:

$$m_2h_2 + m_4h_4 = m_3h_3 + m_5h_5 \tag{14}$$

Where:

m_2, m_3, m_4, m_5: The mass flow rate at points 2, 3, 4, and 5 (kg/s).

The temperature at point 3 is an input value, and since the mass fraction for points 1 to 3 is the same, the enthalpy at this point (h_3) is determined. Actually, the state at point 3 may be sub-cooled liquid. However, at the conditions of interest, the pressure has an insignificant effect on the enthalpy of the sub-cooled liquid, and the saturated value at the same temperature and mass fraction can be an adequate approximation. The enthalpy at point 2 is determined from an isentropic pump model.

The minimum work input (w) can, therefore, be obtained from:

$$w = m_1 \upsilon_1 (p_2 - p_1) \tag{15}$$

Where:

P2, P1: is the pressure at points 1 and 2 (kPa).

υ_1: is specific volume at point 1 (m³ /kg).

It is assumed that the specific volume (v, m³/kg) of the liquid solution does not change appreciably from point (1)-(2). The specific volume of the liquid solution can be obtained from a curve fit.

_____

Now, the unknown enthalpy value (h_5) at point 5can be obtained from the equation of the energy balance on the solution heat exchanger. The temperature at point 5 can also be determined from the enthalpy value.
Finally, the energy balance on the absorber is:

$$Q_a = m_{10}h_{10} + m_{11}h_{11} + m_6h_6 - m_1h_1 \qquad (16)$$

The heat input to the generator is determined from the energy balance, which is:

$$Q_g = m_4h_4 + m_7h_7 - m_3h_3 \qquad (17)$$

The enthalpy at point 7 can be determined, since the temperature at this point is an input value. In general, the state at point 7 will be superheated water vapor, and the enthalpy can be determined once the pressure and temperature are known.
The condenser heat can be determined from an energy balance, which gives:

$$Q_c = m_7(h_7 - h_8) \qquad (18)$$

Finally, the Coefficient of performance (COP) can be obtained by:

$$COP = \frac{Q_e}{Q_g} \qquad (19)$$

3. SIMULATION OF THE SYSTEM

After working on the mathematical model of the system as previous, any of the simulation programs can be used to write and solve the mathematical equations. Engineering Equation Solver (ESS) has been used as one of the simulation programs in thermodynamics to solve the mathematical model and work on results analysis.
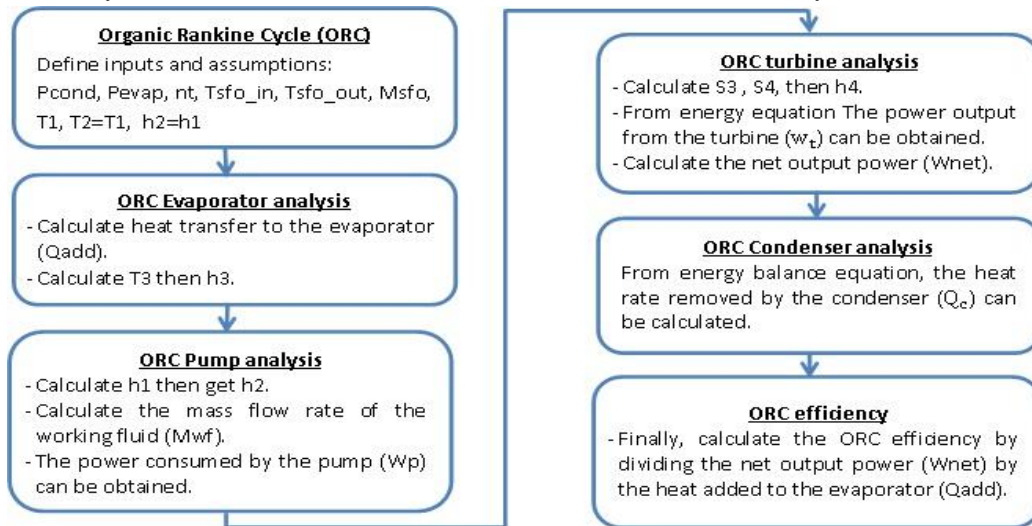
Organic Rankine Cycle (ORC)
Define inputs and assumptions:
Pcond, Pevap, nt, Tsfo_in, Tsfo_out, Msfo, T1, T2=T1, h2=h1

ORC Evaporator analysis
- Calculate heat transfer to the evaporator (Qadd).
- Calculate T3 then h3.

ORC Pump analysis
- Calculate h1 then get h2.
- Calculate the mass flow rate of the working fluid (Mwf).
- The power consumed by the pump (Wp) can be obtained.

ORC turbine analysis
- Calculate S3 , S4, then h4.
- From energy equation The power output from the turbine (w$_t$) can be obtained.
- Calculate the net output power (Wnet).

ORC Condenser analysis
From energy balance equation, the heat rate removed by the condenser (Q$_c$) can be calculated.

ORC efficiency
- Finally, calculate the ORC efficiency by dividing the net output power (Wnet) by the heat added to the evaporator (Qadd).

Fig. 3: ORC program algorithm

Thermal Desorption Chiller (TDC)
Define inputs and assumptions: Qe, T4, X1, X4, T3, T7, T10, and T6=T5, T9=T8, P5=P4, P6=P1, P9=P10

TDC Evaporator analysis
- Calculate P10 and h10, then h11.
- Calculate P4, h4, then h8, and h9.
- From energy and mass balance the mass flow rate at points 9, 10, and 11 are calculated.

TDC Absorber analysis
- From mass balance the mass flow rate at points 1 and 6 are calculated then calculate h1.
- Calculate h3 and h2, then the pump work can be obtained.
- From energy balance h5 can be calculated then h6.
- Now Absorber heat rejected to the environment (Qa) can be obtained.

TDC Generator analysis
- Calculate P7 and T7 then h7.
- From energy balance equation, the heat input to the generator (Qg) is calculated.

TDC Condenser analysis
From energy balance equation, condenser heat rejected to the environment (Qc) is calculated.

TDC COP
Calculate the coefficient of performance (COP) by dividing the cooling capacity (Qe) by the heat input to the generator (Qg).
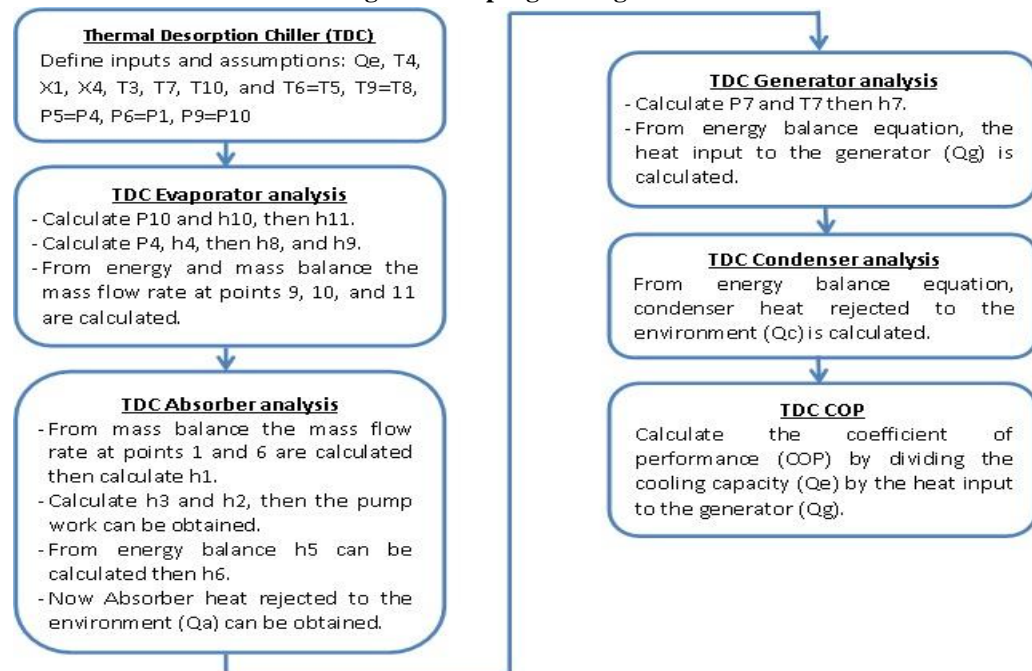
Fig. 4 TDC program algorithm

_____

As shown in figures 3 and 4, the execution the program takes several steps:
- Define inputs and assumptions
- Calculate pressure, temperature, and enthalpy at each point from the cycle
- Obtain the required thermal energy; heat rejected, net output power, and cooling capacity
- Calculate ORC efficiency and TDC coefficient of Performance
- Calculate the cost of both kWh refrigerant and electricity

Donghong Wei et al, [10] studied performance analysis and optimization of ORC for waste heat recovery. The nominal power of this ORC system is 100 kW, the inlet temperature of the exhaust is between 610- 650 K. The properties of the working fluid HFC-245fa are calculated by REFPROP 6.01 [10].
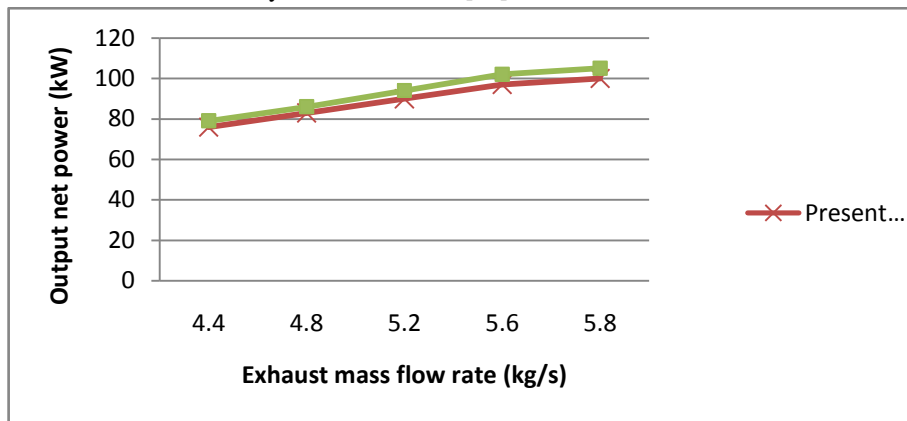
Fig. 5 Output net power vs. exhaust mass flow rate

The present simulation program is loaded by the data of Donghong Wei et al [10] and the output results are shown in Figure 5. Figure 5shows a comparison between the present work and Donghong Wei et al [10] for the output net power versus exhaust mass flow rate work. From this comparison, it is clear that, the two curves have the same trend with some acceptable deviations.

4. Results
After dividing the stored thermal energy into ORC and TDC at different percentages, ORC electric power and TDC cooling capacity are calculated. Figure 6 shows the relation between the input thermal energy of both ORC and TDC and their outputs respectively. With the reference to the following figure, it was noticed that both ORC net output power and TDC cooling capacity increase with the increase of the input thermal energy.
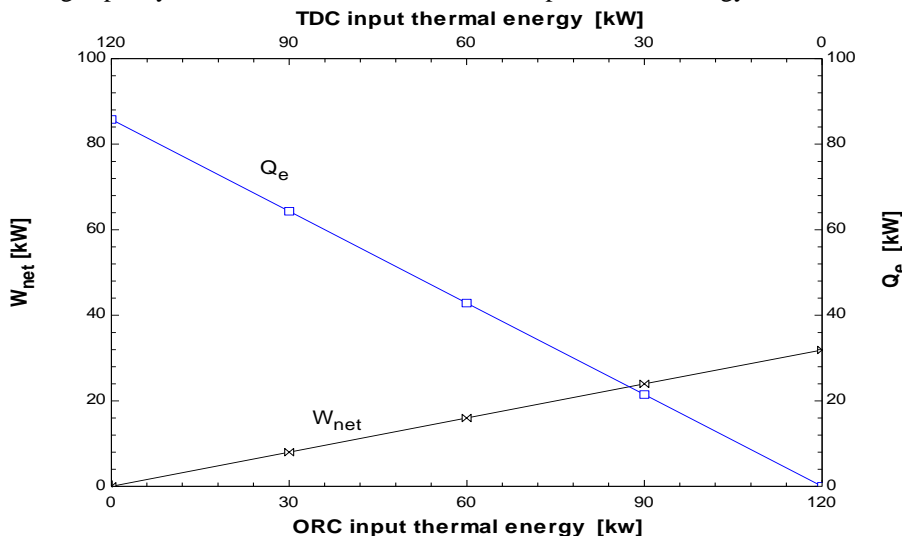

Fig. 6 ORC input thermal energy vs. net output power and the rest of the 120 kW stored energy for TDC vs. cooling capacity

Figure 6 shows that there is an intersection point between the two curves. This intersection point comes at the distribution of the stored thermal energy (120 kW) so that it is 88 kW for ORC and 32 kW for TDC. From this figure, it is clear that, the electrical net output power from ORC is about 24 kW, while the TDC cooling capacity is about 24 kW.

_____

Also, this point is considered the optimum operating conditions, it means the optimum operating conditions occurs when 73.33 % from stored thermal energy is used for ORC and 26.67 % is used for TDC.

4.1. Results of Electrical Load

There are many parameters in the ORC which effect on the output electric power. Here, the effect of inlet hot oil temperature and hot oil mass flow rate on the input thermal energy, net output power, and the ORC efficiency were investigated.

4.1.1. Effect of Inlet Hot Oil Temperature

Figure 7 shows the variation of ORC electric power output, inlet thermal energy, and ORC efficiency versus the inlet hot oil temperature while the outlet hot oil temperature is/isn't constant. As seen in this figure, when the outlet hot oil temperature isn't constant, ORC output electric power decreases with the increase of the inlet hot oil temperature.
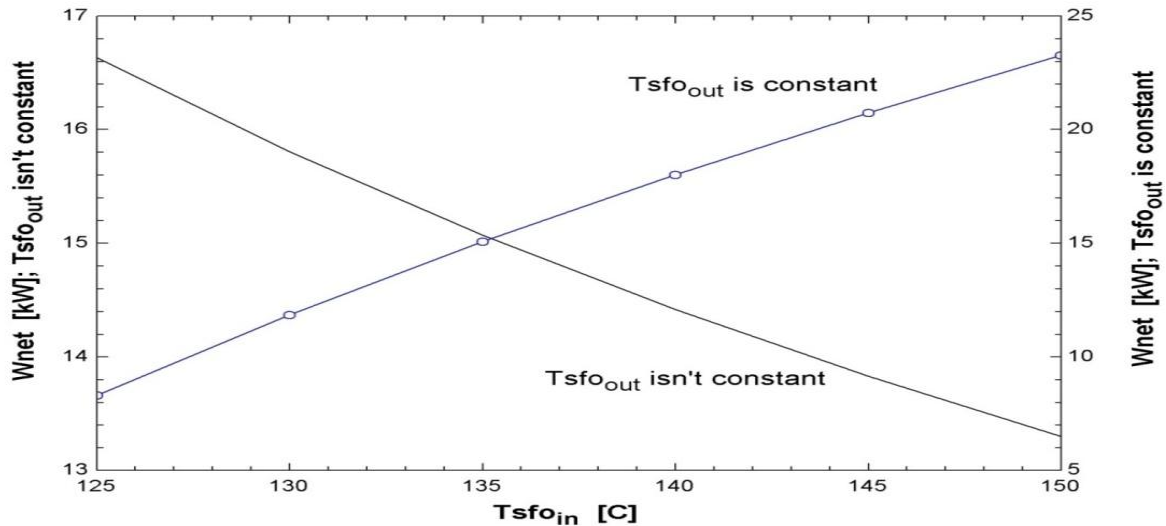
Fig. 7 Inlet hot oil temperature vs. ORC net output power

As shown in figure 7, it is apparent that when the inlet hot oil temperature increases, net electric power increases if the outlet hot oil temperature is constant and net electric power decreases if the outlet hot oil temperature increases. This is because when the inlet hot oil temperature increases and the outlet hot oil temperature is constant, the temperature difference increases, thus increasing the input thermal energy, which increases net electric power. In the case of increasing the temperature of the outlet hot oil with the same increase in the inlet hot oil temperature, the input thermal energy is constant and net electric power is affected only by the variation of evaporator temperature in the cycle. Figure 7 dealt with the effect of the inlet hot oil temperature when R123 is used as a working fluid. Figure 8 shows the same case but for different working fluids. As seen from this figure, all working fluids give the same linearity. Net electric power increases with the increasing of the inlet hot oil temperature. Also, R423a gives higher net electric power and R123 gives lower net electric power.
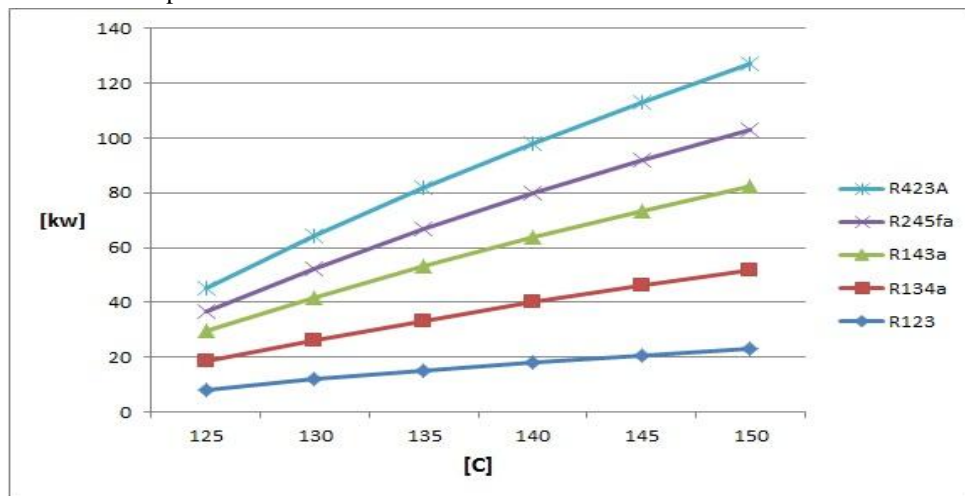

Fig. 8 Inlet hot oil temperature vs. ORC net output power at different working fluids

_____

4.1.2. Effect of Hot Oil Mass Flow Rate:

Figure 9 shows the effect of the mass flow rate of the hot oil (M_{sfo}) on both the input thermal energy and net output power. From this figure, it is clear that increasing mass flow rate increase both the input thermal energy and net output power.
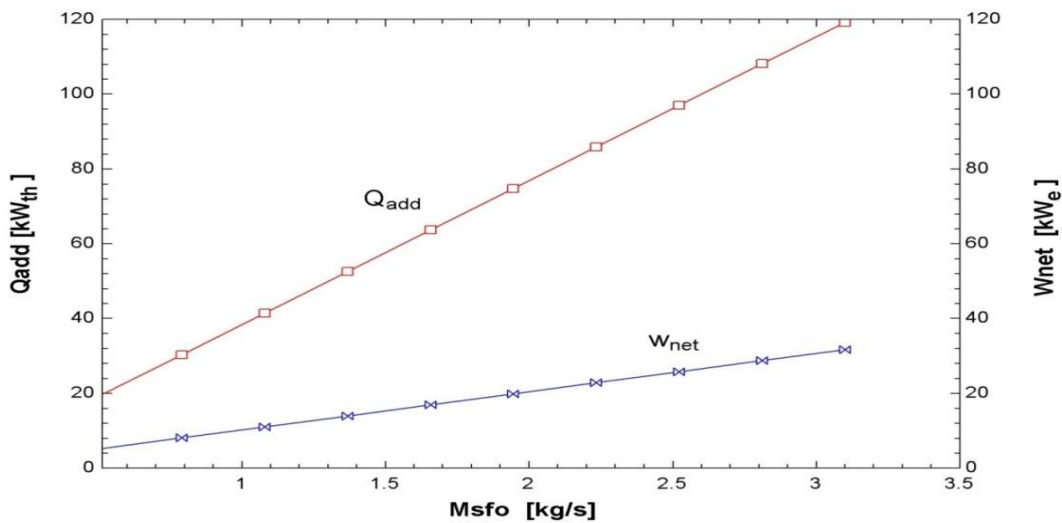

Fig. 9 Hot oil mass flow rate vs. input thermal energy and net output power from ORC

4.2. Results of Cooling Load

There are many parameters in the thermal driven absorption chiller (TDC) modeling which effect on the coefficient of performance (COP) like the effect of generator and evaporator temperatures.

4.2.1. Effect of Generator Temperature

Increasing input thermal energy is definitely offset by an increasing in the generator temperature. This statement is confirmed by figure 10 which illustrates the effect of the generator temperature on both the input thermal energy and coefficient of performance.
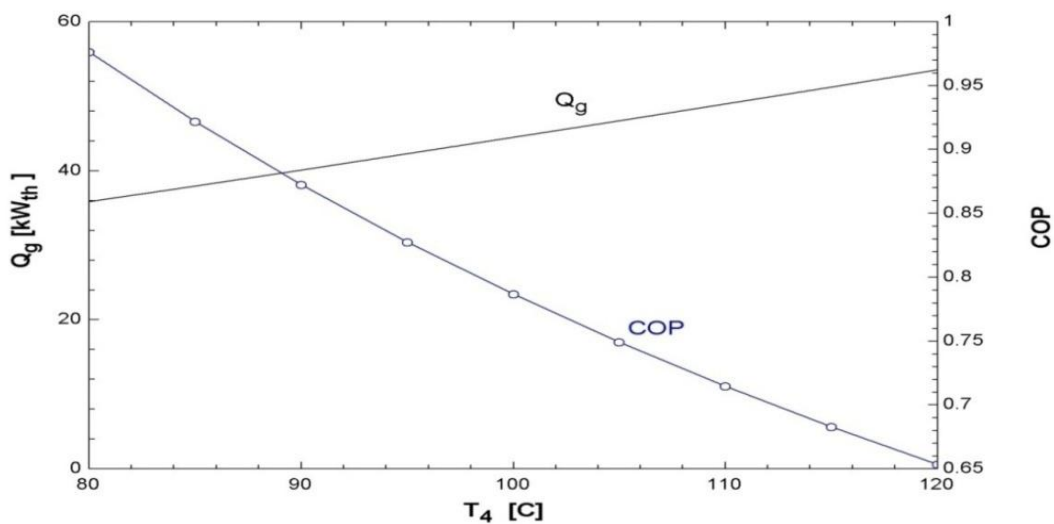

Fig. 10 Generator temperature vs. input thermal energy and COP (TDC)

As shown from figure 10, with the generator temperature increasing, the input thermal energy increases. This is because of in order to obtain a higher generator temperature; the input thermal energy must be increased. Also, when the generator temperature is increased, the generator pressure is also increased, and this has the effect of lowering the COP of the unit, considering that the pressures and temperatures at other points of the unit are kept constant.

4.2.2. Effect of Evaporator Temperature

Figure 11 shows the effect of evaporator temperature on the required thermal energy and the coefficient of performance of the system. It can be seen that required thermal energy gradually decreases with the increase in evaporator temperature, thus increasing the coefficient of performance.
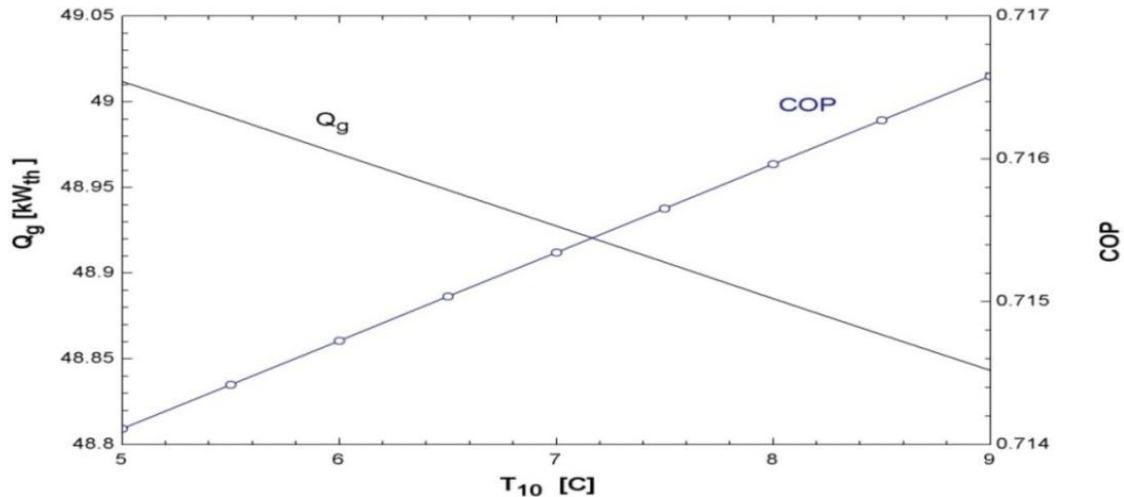
_____

Fig. 11 Evaporator temperature vs input thermal energy and COP (TDC)

5. CONCLUSION

Referring to the analysis of the results after simulate the proposed system which consists of solar collector field of 120 kW peak thermal capacity, thermal storage tank with 3 tons of therminol-66 oil, an Organic Rankine Cycle (ORC) of 4.3 kW nominal electric power production capacity, and thermally driven absorption chiller (TDC) of 35 kW cooling capacity. The following conclusion points are obtained:

- When the exit temperature is constant, the ORC output electric power and inlet thermal energy increase with the increase of the inlet hot oil temperature while decreasing the overall ORC efficiency. When applying different working fluids, the same linearity was found but at higher electric output power.
- At different working fluids, the net electric power also increases with the increase of the inlet hot oil temperature. In addition to that R423a gives higher net electric power and R123 gives lower net electric power.
- When the exit temperature isn't constant, the ORC output electric power decreases with the increase of the inlet hot oil temperature.
- As it becomes clear in ORC that with increasing mass flow rate, both the input thermal energy and net output power increase.
- Increasing input thermal energy to TDC is definitely offset by an increasing in the generator temperature.
- When the generator temperature is increased, the generator pressure is also increased, and this has the effect of lowering the COP of the unit, considering that pressures and temperatures at other points of the unit are kept constant.
- It can be seen that COP gradually increases with the increase in evaporator temperature values.
- At optimum operating condition, the electrical net output power from ORC is about 24 kW, while the TDC cooling capacity is about 24 kW. The optimum operating conditions occurs when 73.33 % from stored thermal energy is used for ORC and 26.67 % is used for TDC.

REFERENCES

[1].   R. C. Bansal, T. S. Bhatti, and D. P. Kothari, "Bibliography on the application of induction generators in nonconventional energy systems", IEEE transactions on energy conversion, vol. 18, no. 3, (2003).
[2].   L. Chang and H.M. Kojabadi, "Review of interconnection standards for distributed power generation", Large Engineering Systems Conference on Power Engineering (LESCOPE' 02), pp. 36 - 40, (2002).
[3].   Umberto Desideri, Pietro Elia Campana, "Analysis and comparison between a concentrating solar and a photovoltaic power plant", Applied Energy, vol. 113, pp. 422–433, (2014).
[4].   Wisam Abed Kattea Al-Maliki, Falah Alobaid, Vitali Kez, Bernd Epple, "Modeling and dynamic simulation of a parabolic trough power plant", Journal of Process Control, vol. 39, pp. 123–138, (2016).
[5].   Monica Borunda, O.A. Jaramillo, R. Dorantes, Alberto Reyes, "Organic Rankine Cycle coupling with a Parabolic Trough Solar Power Plant for cogeneration and industrial processes", Renewable Energy, vol. 86, pp. 651-663, (2016).
[6].   Mustapha Merzouk, Nachida Kasbadji Merzouk, Said El Metenan, Omar Ketfi, "Performance of a Single Effect Solar Absorption Cooling System (Libr-H2O)", Energy Procedia, vol. 74, pp. 130 – 138, (2015).

_____

[7]. Mohamed H. Ahmed, Mohamed A. Rady and Amr M. A. Amin, "Multi Applications of Small Scale Solar Power Plant Using Organic Rankine Cycle and Absorption Chiller", 2014.

[8]. G.A. Florides, S.A. Kalogirou, S.A. Tassou, L.C. Wrobel, "Design and construction of a LiBr−water absorption machine", Energy Conversion and Management, vol. 44, pp. 2483–2508, (2003).

[9]. M. Astolfi, L. Xodo, M. C. Romano, E. Macchi, Technical and economic analysis ofa solar-geothermal hybrid plant based on an Organic Rankine Cycle, vol. 40, pp. 58-68, (2010).

[10]. Donghong Wei, Xuesheng Lu, Zhen Lu, Jianming Gu, "Performance analysis and optimization of organic Rankine cycle (ORC) for waste heat recovery", Energy Conversion and Management, vol. 48, pp. 1113−1119, (2007).